Article

High-Hardness, Water-Stable, and UV-Resistant Conductive Coatings Based on Waterborne PEDOT:PSS/Epoxy/(KH560/SiO$_2$) Composite

Zhanqi Li [1], Ling Zhu [2], Xiaowen Xie [2], Meng Zhou [2], Changqing Fu [2,*] and Shuai Chen [1,2,*]

1   School of Chemistry and Chemical Engineering, Jiangxi Science and Technology Normal University, Nanchang 330013, China
2   Jiangxi Engineering Laboratory of Waterborne Coatings, Nanchang 330013, China
*   Correspondence: fuchq0791@163.com (C.F.); shuaichen@jxstnu.edu.cn (S.C.)

Abstract: Despite the fact that PEDOT:PSS has been successfully used in the field of flexible electronics, some of its applications in the domain of rigid conductive coating have been limited by the pricey cost and subpar mechanical properties (hardness, adhesion, and moisture absorption) of the commercially available Clevios™ PH 1000, as well as the poor conductivity, film formation, and mechanical properties of the self-made PEDOT:PSS. In the process of investigating the low-cost preparation of PEDOT-based conductive polymer coatings, we discovered that self-made PEDOT:PSS, a waterborne epoxy resin, and a bio-based epoxy curing agent can be blended uniformly to produce good film-forming conductive coatings. Later, the addition of KH560-modified nano-SiO$_2$ further improved the coating's hardness while ensuring a modest increase in conductivity. Meanwhile, the inadequacies of the epoxy resin, which are not UV-resistant, were considerably improved by the synergistic action of PEDOT:PSS and the modified SiO$_2$. The result is a low-cost method designed for creating conductive coatings that are UV-resistant and may be utilized for electromagnetic, electrothermal, and antistatic shielding applications. Such a PEDOT:PSS/epoxy composite system and its design approach will broaden the scope of PEDOT:PSS's application and will inspire future research in and practical implementations of PEDOT:PSS-based conducting coatings.

Keywords: waterborne epoxy resin; PEDOT:PSS; high hardness; conductive coatings; bio-based; UV-resistant

1. Introduction

Intrinsically conducting polymers (ICPs) have emerged as one of the most promising electronic materials due to their low toxicity, high environmental stability, and ease of synthesis. Among them, poly(3,4-ethylenedioxythiophene):polystyrene sulfonate (PEDOT:PSS) as one of the most successful conductive polymers, due to its tunable conductivity, excellent thermal stability, flexibility, and other characteristics, has been widely used in wearable electronics [1], transistors [2], sensors [3], photovoltaic devices [4], and many other practical applications. However, both commercial and self-made PEDOT:PSS aqueous dispersions have poor mechanical properties after film formation, and the films are prone to moisture absorption [5], brittleness, and cracking [6], resulting in impaired performance, which limits the electronic application of their films. Therefore, the development of organic electronic films with high mechanical properties and environmental stability is a current research hotspot.

Typically, PEDOT:PSS is coated on a flexible substrate such as polydimethylsiloxane (PDMS) [7], polyethylene terephthalate (PET) [8], or polyimide (PI) [9] or directly mixed with elastomers such as polyurethane [10], cellulose [11], etc., but the filler content in the blend elastomer/conductive polymer also affects its electrical properties, as well as other

parameters such as substrate adhesion, mechanical properties, etc. Recently, the combination of PEDOT:PSS and environmentally friendly resins has been reported to improve the mechanical properties and environmental stability of its overall composites [12,13]. These papers, however, continue to focus on flexibility as a way to improve the mechanical qualities of PEDOT:PSS composites.

In comparison, waterborne epoxy resins are inexpensive, non-toxic, and eco-friendly non-flexible synthetic resins that, when cured with a curing agent, display good mechanical qualities and offer the substrate exceptional protection [14,15]. The utilization of bio-based resources, such as cashew phenol and castor oil, to manufacture bio-based epoxy resins or curing agents is becoming increasingly sophisticated as environmental protection continues to grow [16]. Recently, waterborne epoxy resin technology have become a very established field. The commercialization of several bio-based waterborne epoxy emulsions and curing agents has already occurred, which has received widespread attention. They provide an abundant and affordable raw material for combination with aqueous ICPs. However, its own weak anti-ultraviolet ability is its inevitable shortcoming. Due to the instability of its aromatic skeleton, epoxy coatings are subject to gloss loss, yellowing, and even chalking when exposed to sunshine or UV radiation over an extended length of time and eventually lose their capacity to shield the substrate [17–19].

However, a unique optical property against UV light is one of the numerous special characteristics of nanoscale silica. Since it is non-toxic and ecologically benign, it is frequently used as a filler in organic coatings to increase the durability, strength, and chemical resistance of other polymers materials. This also helps to reduce the need for coating film-formers and, consequently, material costs. Similarly, extensive research has been conducted on the mechanical characteristics of polymers reinforced with various nanofillers or fibers [20]. Nanoscale silica, on the other hand, is prone to agglomeration, and its homogeneity in polymer dispersions can be enhanced by altering its surface with a silane coupling agent [21,22] or by vigorous homogenization.

In this study, we created a pre-dispersion by combining a waterborne epoxy emulsion with a bio-based epoxy curing agent, which was then combined with a self-made PEDOT:PSS to create coatings with various PEDOT:PSS/epoxy solid ratios (P:E ratios were used below). Then, we investigated the addition of various levels of modified nano-silica (KH560/SiO$_2$) to the dispersion at a P:E ratio of 1:4, which further decreased the cost of the coating and improved its hardness to a certain extent. Even while PEDOT:PSS by itself has a strong UV resistance [23], the ternary system (PEDOT:PSS/epoxy/(KH560/SiO$_2$), P:E:K ratios were used below) was created by mixing it with modified SiO$_2$ and pre-dispersion, while PEDOT:PSS and KH560/SiO$_2$ further reduce the susceptibility of the coating to UV aging. Meanwhile, epoxy resin serves as a film-former and gives the coating its fundamental mechanical qualities. The end result is a production-ready, cost-effective, UV-resistant, waterborne conductive coating that has been prepared in an ecologically benign manner.

2. Materials and Methods

2.1. Materials

Polystyrene sulfonate sodium salt (PSS-Na, 99%, Mw = 500,000) was purchased from Alfa Aesar (China) Chemical Co., Ltd., Shanghai, China. Concentrated hydrochloric acid (HCl, AR grade) was purchased from Shanghai Reagent Chemical Co., Ltd., Shanghai, China. Sodium hydroxide (NaOH, AR grade) was purchased from Shanghai Vita Chemical Reagent Co., Ltd., Shanghai, China. Silicon dioxide (hereinafter still referred to SiO$_2$, 99.5%, 30 nm), ammonia solution (NH$_3$·H$_2$O, CP grade, ≥25% in H$_2$O), 3,4-ethylenedioxythiophene (EDOT, 99%), 717# anion exchange resin, 732# cation exchange resin, and 3-glycidyloxypropyltrimethoxysilane (KH560, C$_9$H$_{20}$O$_5$Si, 97%, Figure 1) as a silane coupling agent (SCA) were purchased from Aladdin Reagent (Shanghai, China) Co., Ltd. Sodium persulfate (Na$_2$S$_2$O$_8$, AR grade) was purchased from Sinopharm Group Chemical Reagent Co., Ltd., Shanghai, China. Anhydrous ferric sulfate (Fe$_2$(SO$_4$)$_3$, AR grade) was purchased from Tianjin Hengxing Chemical Reagent Manufacturing Co., Ltd., Tianjin,

China. The waterborne epoxy emulsion (WR 2253, Bisphenol A epoxy resin, abbreviated as DGEBA, Table S1) and biobased waterborne epoxy amine curing agent (WRH 6765) were all provided by Beijing Mytimes Trading Co., Ltd., Beijing, China. Dichloromethane (DCM, 99%) and anhydrous ethanol (EtOH, 99%) were provided by Shanghai Titan Technology Co., Ltd., Shanghai, China. Acetone (AR) was purchased from Sinopharm Group Chemical Reagent Co., Ltd., Shanghai, China. Deionized (DI) water was all laboratory-made by a ultrapure water device (UPT-11-100T) provided by Sichuan ULUPURE Ultrapure Technology Co., Ltd., Chengdu, China. All reagents and chemicals were used without further purification. The physical and chemical characteristics of the primary raw materials employed in the studies are listed in Table S1.
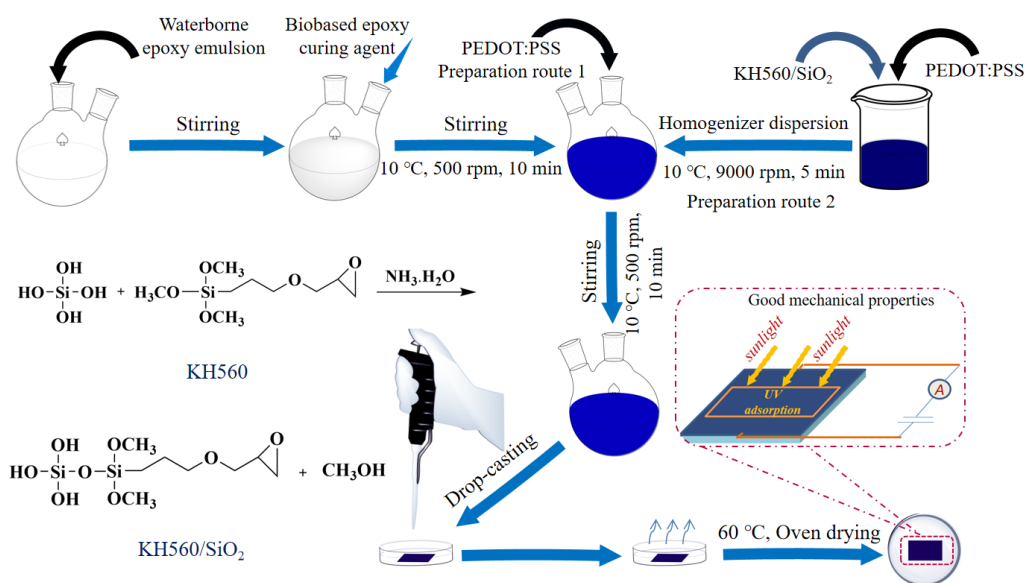

Figure 1. Schematic illustration of the preparation process of PEDOT:PSS/epoxy (route 1) and PEDOT:PSS/epoxy/(KH560/SiO$_2$) (route 2) aqueous dispersions, coatings, and the synthetic route of KH560/SiO$_2$.

2.2. Preparation of KH560/SiO$_2$

In order to modify the silica nanoparticles, the reported methods have been employed [24]: 180 mL of EtOH and 50 mL of DI water suspension with 3 g of SiO$_2$ were added into the 500 mL two-necked flask with a stirrer and a condenser. After stirring for 0.5 h, the pH value was adjusted to 9–10 by adding an NH$_3$·H$_2$O solution. Then, the oil bath temperature was increased to 80 °C for the subsequent reaction. Next, a mixture of 3 g of the organic silane coupling agent (KH560) and EtOH was poured into the flask slowly and left to react for 4 h at 80 °C. Finally, KH560/SiO$_2$ was obtained after centrifuging (Desktop high speed centrifuge, HG1650, Hunan Xiang Yi Laboratory Instrument Development Co., Ltd., China, 8000 rpm), washing to neutral pH with EtOH and DI water several times, and drying in an oven to remove moisture. The synthetic route of KH560/SiO$_2$ is given in Figure 1.

2.3. Preparation of PEDOT:PSS-Based Composite System
2.3.1. Preparation of PEDOT:PSS Aqueous Dispersion

To prepare the self-made PEDOT:PSS aqueous dispersion, the optimized chemical oxidation polymerization method reported by our group was adopted [25]. In detail, 1.458 g (2.886 μmol) of PSS-Na was dispersed into 26.38 mL of DI water in a two-necked flask. The appropriate amount of HCl solution (1 mol/L) was added to control the pH value of the aqueous system to about 0–1; then, the mixture was stirred mechanically at 25 °C until the PSS-Na completely dissolved. Next, 0.5241 g (3.647 mmol) of EDOT, 7.100 mg (17.76 μmol)

of $Fe_2(SO_4)_3$, and 1.007 g (4.187 mmol) of $Na_2S_2O_8$ were added under a stirring state and further stirred at 25 °C for 24 h. The synthesized mixture was treated with 717# anion and 732# cation exchange resins, suction filtered (Sand core funnel, G3, Chongqing Synthware Glass Co., Ltd., Chongqing, China) to separate large-sized PEDOT:PSS aggregates and the ion exchange resins, and then taken out for rotary evaporation to control its solid content to 1.52 wt.%. The prepared dark-blue PEDOT:PSS aqueous dispersion had a viscosity of 21.5 mPa·s (Digital viscometer NDJ-5S, Shanghai Hengping Instrument Factory, Shanghai, China; 26 °C) and pH value of 1.72 (pH meter PHS-3CB, Shanghai Yueping Scientific Instrument Co., Ltd., Shanghai, China, 26 °C).

2.3.2. Preparation of PEDOT:PSS/Epoxy and PEDOT:PSS/Epoxy(KH560/SiO$_2$) Composite

　　As shown in Figure 1 (route 1), the PEDOT:PSS/epoxy aqueous dispersion was pre-pared by adding a waterborne epoxy emulsion system into the PEDOT:PSS aqueous dispersion (10.00 ± 0.02 g) under mechanical stirring (500 rpm, 10 °C) for 10 min. The former was pre-prepared by mixing a biobased amine curing agent, waterborne epoxy, and DI water under a mass ratio of 10:1 according to the manufacturer's recommendation to control its solids ratio to 39.1 wt.% and at 10 °C, avoiding too fast of a cross-linking and curing. Besides pristine PEDOT:PSS and pure epoxy (i.e., P:E ratio = 1:0 and 0:1), the P:E ratios of PEDOT:PSS/epoxy were adjusted to 1:1, 1:2, 1:3, 1:4, 1:5, 1:6, 1:7, 1:8, 1:9, and 1:10. As shown in Figure 1 (route 2), PEDOT:PSS/epoxy/(KH560/SiO$_2$) (P:E ratio = 1:4) aqueous dispersions were prepared by adding the pre-prepared waterborne epoxy emul-sion (500 rpm, 10 °C, 10 min) into the pre-mixed (using homogenizer; 9000 rpm, 10 °C, 5 min) aqueous dispersion of PEDOT:PSS (10.00 ± 0.02 g) with KH560/SiO$_2$ and then further stirred (500 rpm, 10 °C) for 5 min. the P:E:K ratios were adjusted to 1:4:0.05, 1:4:0.10, 1:4:0.15, 1:4:0.20, 1:4:0.25, and 1:4:0.30.

2.4. Preparation of PEDOT:PSS/Epoxy and PEDOT:PSS/Epoxy/(KH560/SiO$_2$) Composite Coatings

　　As shown in Figure 1, the PEDOT:PSS/epoxy and PEDOT:PSS/epoxy/(KH560/SiO$_2$) coatings were prepared by dispensing their aqueous dispersions onto the surfaces of the pre-treated soda-lime glass substrate (2 × 2 cm, 5 × 10 cm), which was spread out evenly, and by drying in an oven at 60 °C for 6 h. The modification of the soda-lime glass surfaces was carried out by cleaning them via ultrasonic treatment by reagents in the following order: DCM, EtOH, acetone, DI water, and EtOH, each for 10 min. Following the same method, the pristine PEDOT:PSS coatings were prepared for comparison. Finally, the dried PEDOT:PSS and its cured composite coatings with a thickness of 0.04–0.06 mm were prepared.

2.5. Characterizations

2.5.1. Microstructure and Morphology

　　The thermal stabilities of SiO$_2$ and modified SiO$_2$ (Figure 2) were measured by TGA (TG 209 F3, Netzsch Scientific Instrument Trading (Shanghai) Co., Ltd., Shanghai, China), and the samples were placed in a nitrogen atmosphere with a heating rate of 10 °C min^{-1} from 40 °C to 800 °C. Fourier transform infrared (FT-IR) spectroscopy (Nicolet iS5, ThermoFisher Technology (China) Co., Ltd., Shanghai, China) was used to mea-sure the structure of SiO$_2$, KH560/SiO$_2$ (Figure 3) in the range from 4000 to 400 cm^{-1} with the KBr tablet. Sample photos of the waterborne epoxy emulsion, biobased cur-ing agent, and PEDOT:PSS/epoxy aqueous dispersions (Figure S1) were collected with a Xiaomi 10Pro, Xiaomi Corporation, Beijing, China. The surface microscope morphol-ogy of the pristine PEDOT:PSS (Figure 4), PEDOT:PSS/epoxy (Figures 4 and 5), and PEDOT:PSS/epoxy/(KH560/SiO$_2$) (Figures 6 and 7) coatings was provided by a metallur-gical microscope from the top and bottom light sources (LW300LJT, Beijing Cewei Optoelec-tronic Technology Co., Ltd., Beijing, China). The surface morphology and EDS mapping (S and Si elements) of the PEDOT:PSS/epoxy and PEDOT:PSS/epoxy/(KH560/SiO$_2$) coatings (Figure 8) were recorded using scanning electron microscopy (SEM, Regulus 8100, Hitachi,

Tokyo, Japan) and a energy dispersive spectrometer (EDS, Octane Elect Super—70 mm^2, EDAX(China), Beijing, China). The molecular structures of pristine PEDOT:PSS, cured epoxy, uncured epoxy, and PEDOT:PSS/epoxy (Figure 9) were measured using an FT-IR spectrometer (Nicolet S20, ThermoFisher). Coating thickness was measured by a thickness gauge (Electronic digital caliper 605-01, Genertec Harbin Measuring & Cutting Tool Group Co., Ltd., Harbin, China).
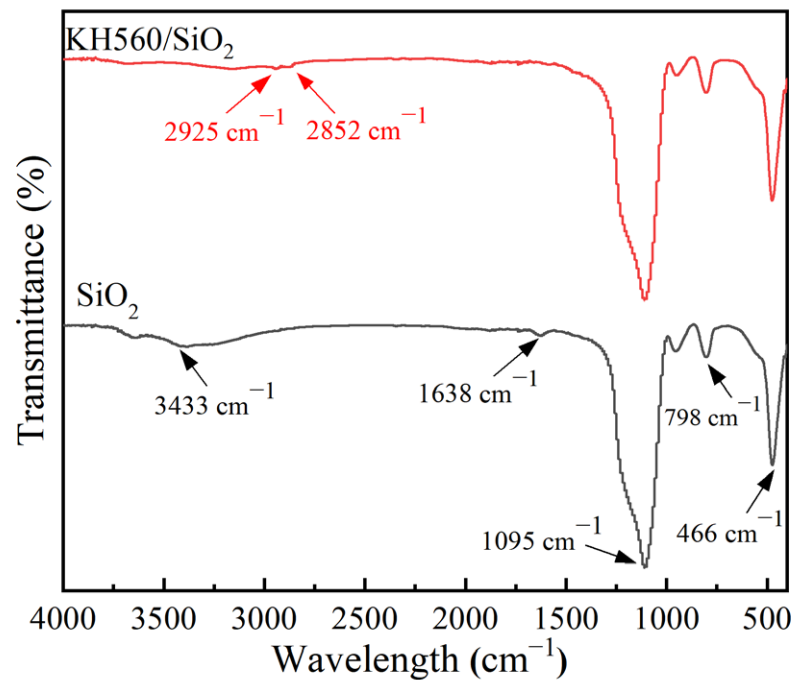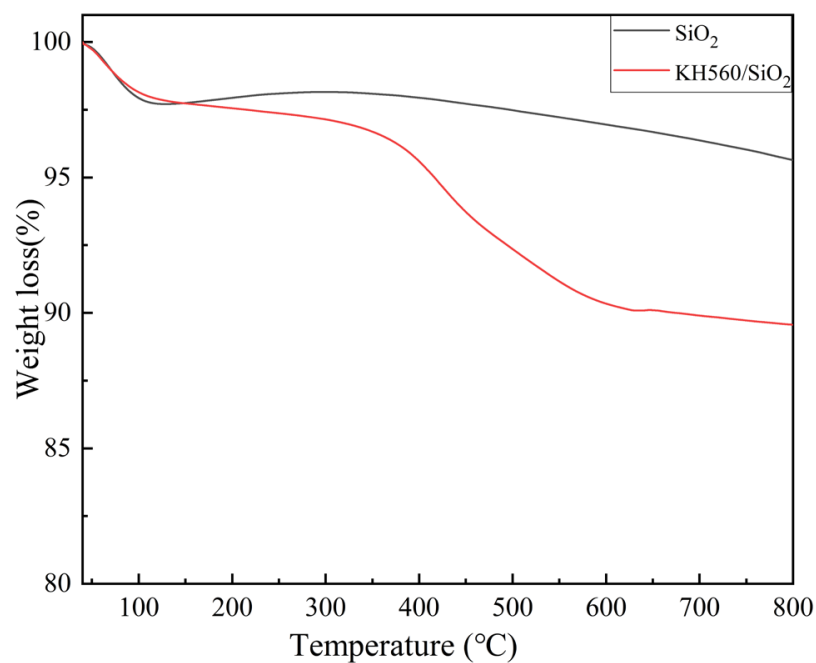

Figure 2. FT-IR patterns of SiO$_2$ and KH560/SiO$_2$.

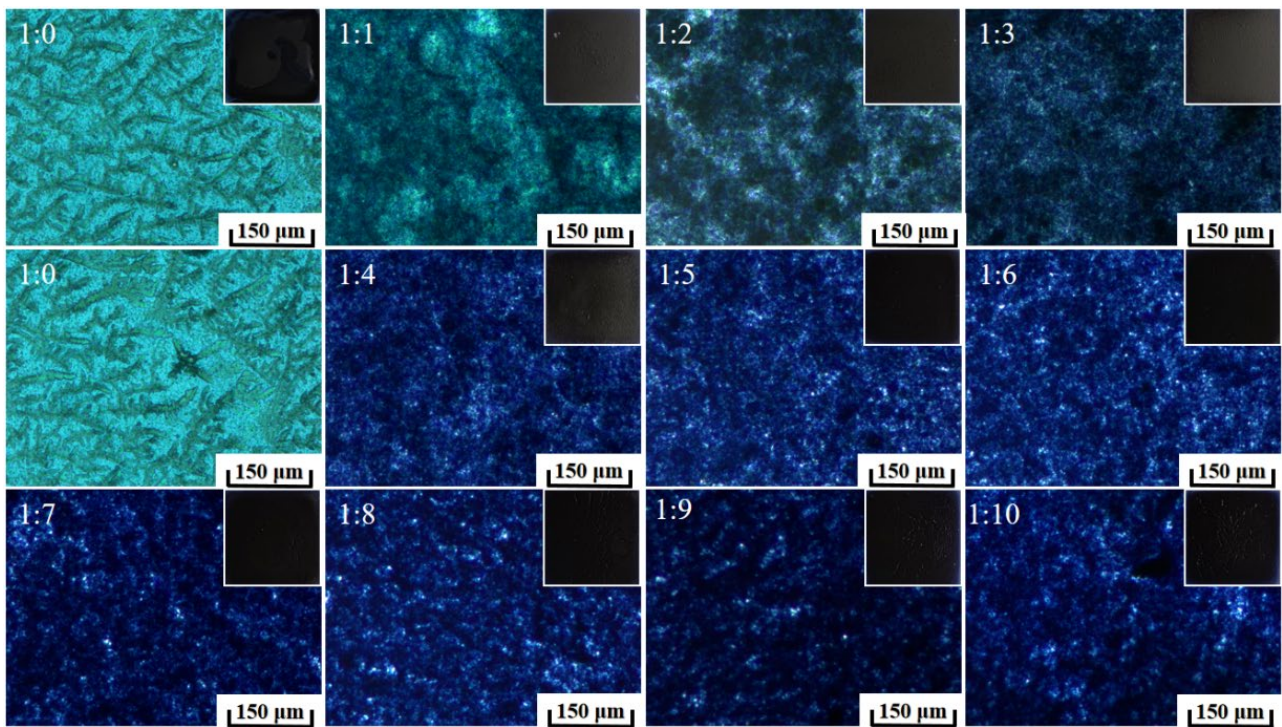**Figure 3.** TGA curves of SiO$_2$ and KH560/SiO$_2$.

Figure 4. Microscope morphology photos of PEDOT:PSS/epoxy coatings (bottom light source) with different P:E ratios and their sample images.

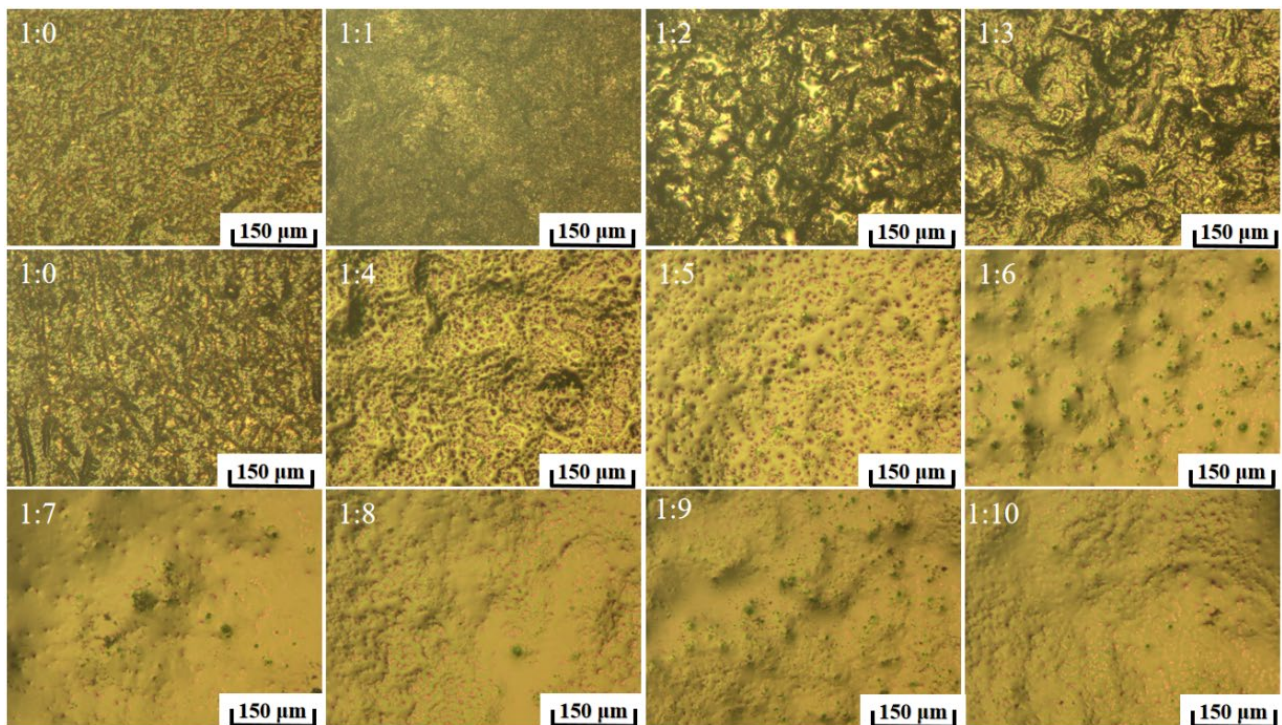**Figure 5.** Microscope morphology photos of PEDOT:PSS/epoxy coatings (top light source) with different P:E ratios.
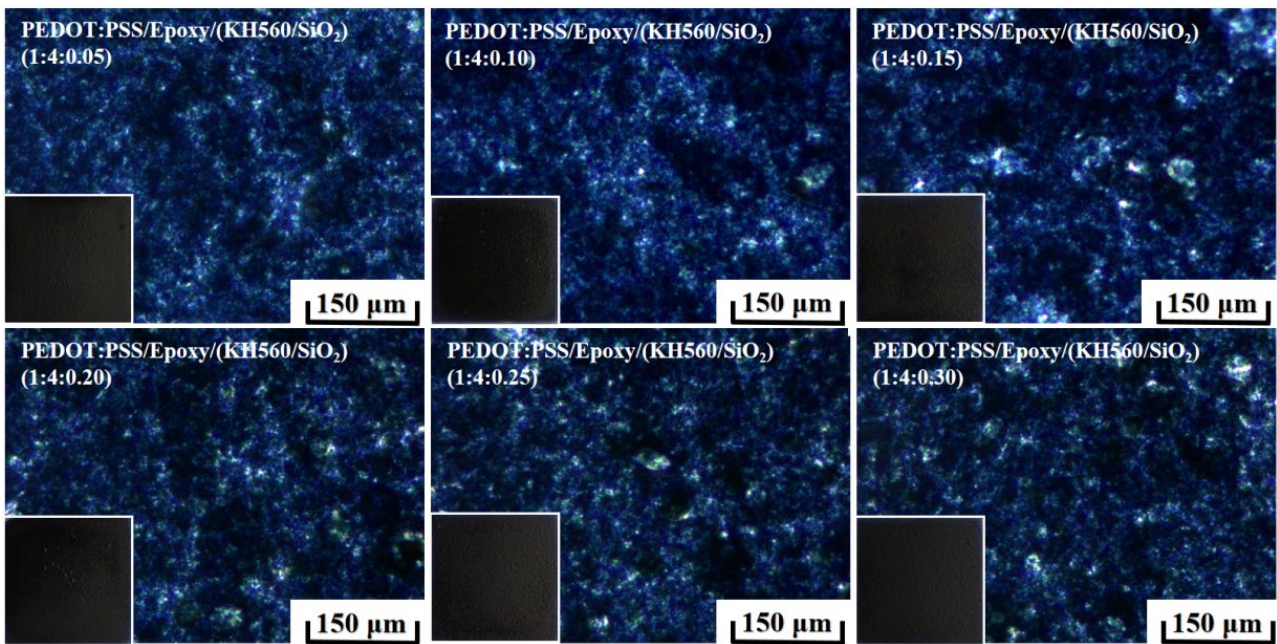
Figure 6. Microscope morphology photos of PEDOT:PSS/epoxy/(KH560/SiO$_2$) coatings (bottom light source) with different P:E:K ratios and their sample images.
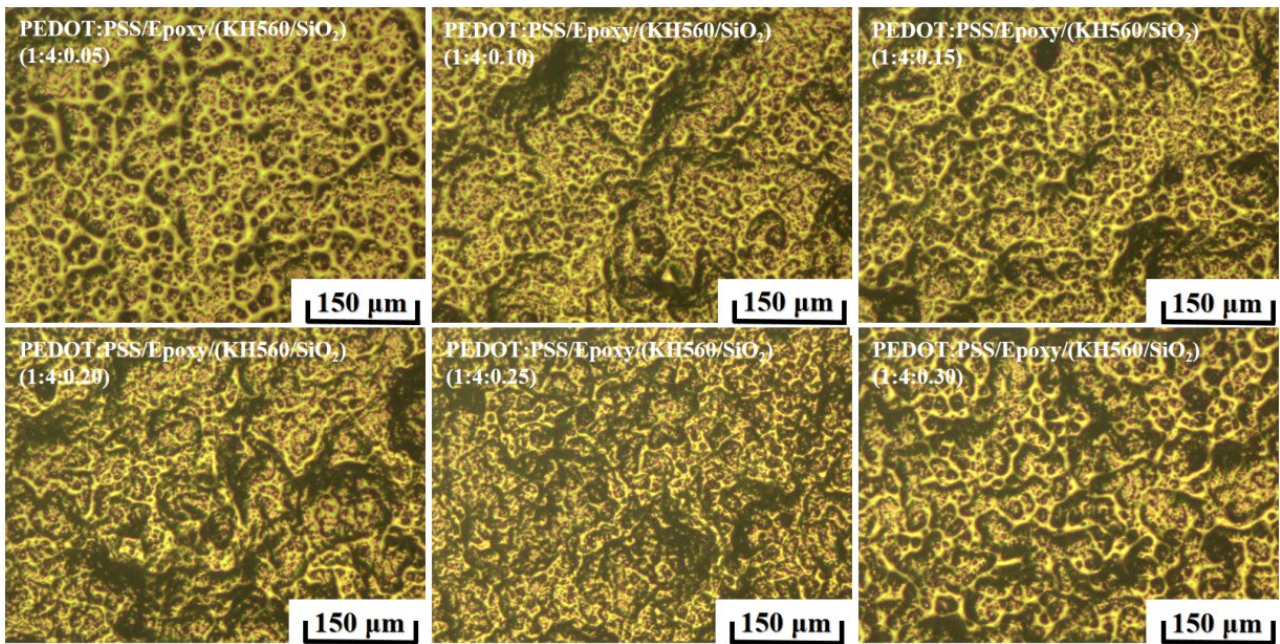

Figure 7. Microscope morphology photos of PEDOT:PSS/epoxy/(KH560/SiO$_2$) coatings (top light source) with different P:E:K ratios.
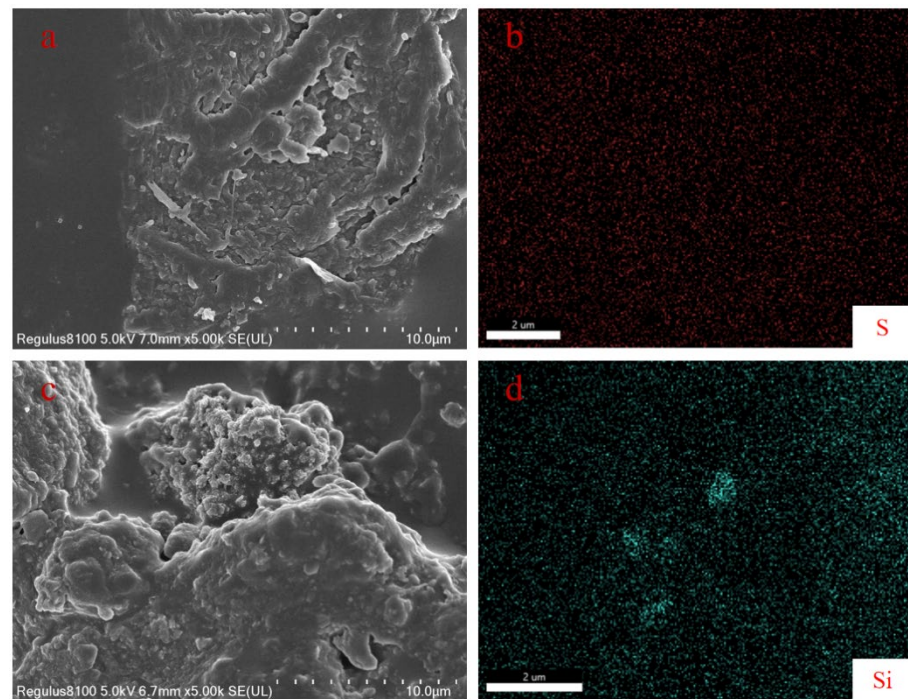
Figure 8. SEM images of PEDOT:PSS/epoxy coating (P:E = 1:4) (**a**) and PEDOT:PSS/epoxy/(KH560/SiO$_2$) coating (P:E:K = 1:4:0.15) (**c**). EDS mapping (S and Si elements) images of PEDOT:PSS/epoxy coating (P:E = 1:4) (**b**) and PEDOT:PSS/epoxy/(KH560/SiO$_2$) coating (P:E:K = 1:4:0.15) (**d**).
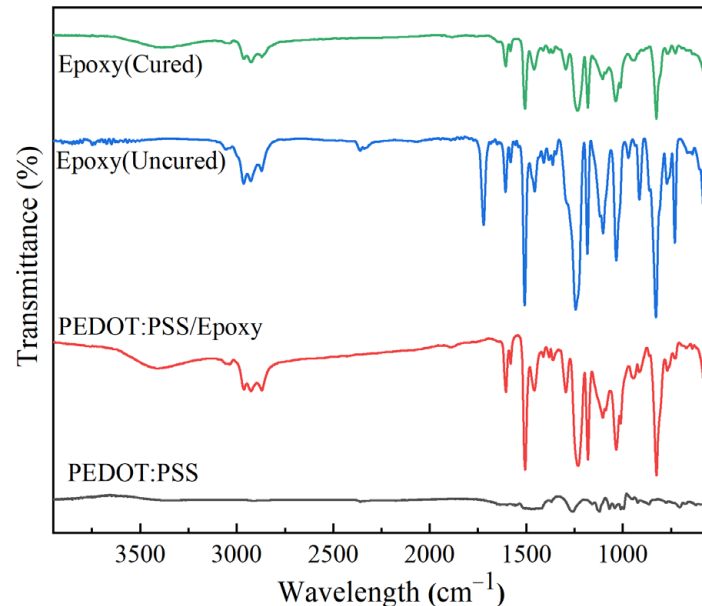
Figure 9. Infrared spectra of epoxy (cured), epoxy (uncured), pristine PEDOT:PSS, and PEDOT:PSS/epoxy coatings.

2.5.2. Bulk Resistance

The conducting behaviors of the PEDOT:PSS/epoxy (Figures 4 and 5) and PEDOT:PSS/epoxy/(KH560/SiO$_2$) (Figures 6 and 7) coatings were evaluated by their bulk resistance (Figure 10) via a two-point probe method in which both ends of the coating were clamped with electrodes using a Keithley 2100 Source Meter, Tektronics (China), Shanghai, China.

Figure 10. Bulk resistance of PEDOT:PSS/epoxy (**a**) and PEDOT:PSS/epoxy/(KH560/SiO$_2$) (**b**) coatings.

2.5.3. Surface Wettability and Water Resistance Stability

The surface wettability of the PEDOT:PSS/epoxy (Figure 11a) and PEDOT:PSS/epoxy/(KH560/SiO$_2$) (Figure 11b) coatings was determined by measuring their water contact angles (WCAs) at ambient conditions (25 ± 3 °C and 50% relative humidity) using a contact angle goniometer (SDC-100, Dongguan Shengding Precision Instrument Co., Ltd., Dongguan, China). The final data of the WCAs were the average values of three parallel measurements on differen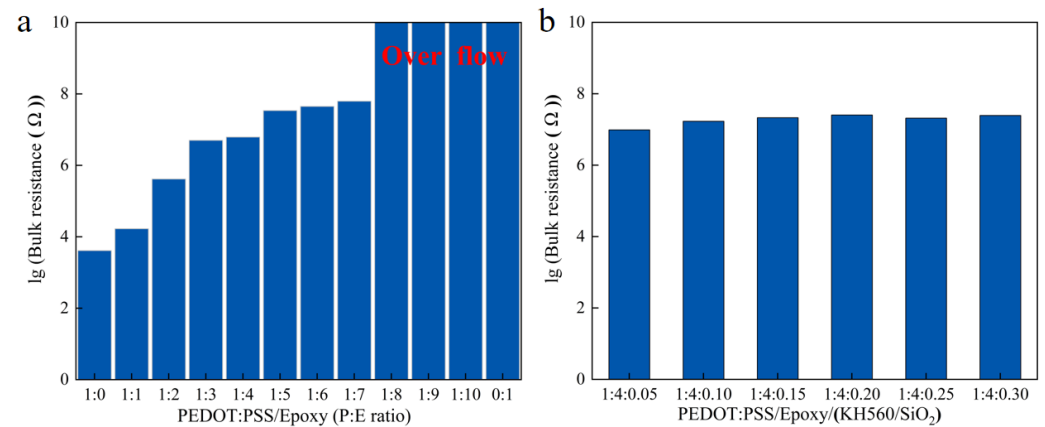t sites of the same coating. The water resistance of the pristine PEDOT:PSS, PEDOT:PSS/epoxy, and PEDOT:PSS/epoxy/(KH560/SiO$_2$) coatings (Figure S2) was studied based on their water immersion stability tests, that is, the coatings were immersed into DI water at 25 °C for 0–10 days to investigate their change in appearance and morphology.
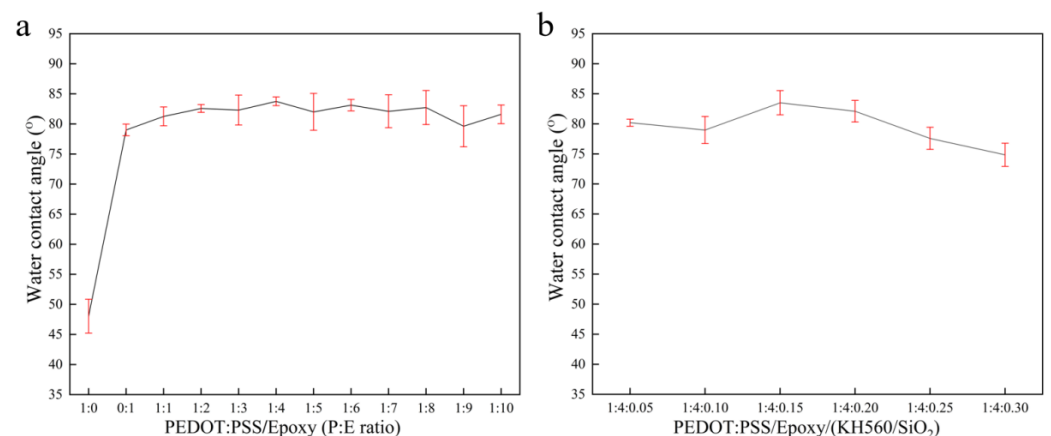
Figure 11. WCAs of PEDOT:PSS/epoxy (**a**) and PEDOT:PSS/epoxy/(KH560/SiO$_2$) (**b**) composite coatings.

2.5.4. Pencil Hardness Property

The pencil hardness properties of the PEDOT:PSS/epoxy and PEDOT:PSS/epoxy/(KH560/SiO$_2$) coatings were determined according to the Chinese National Standard GB/T6739-2006. A pencil scratching meter (Pencil 9800, Mitsubishi, 6B-9H, Tokyo, Japan) was used to divide the hardness grades of these coatings. After fixing a sharpened pencil lead to the trolley (Trolley pencil hardness tester, BGD 506/2, Guang Zhou Biuged laboratory instruments Co., Ltd., Guangzhou, China), it was pushed horizontally over the coatings at a speed of 0.9 mm/s for a distance of at least 7 mm. The hardness of the coatings was determined by observing whether the scratch was less than 3 mm long.

2.5.5. UV Resistant Property

The coatings were irradiated for 15 h per day by placing them in a triple-use UV instrument dark box with UV light (Triple-purpose ultraviolet analyzer, ZF-2, Shanghai Anting Scientific Instrument Factory, Shanghai, China) at 365.0 and 253.7 nm turned on. Aging of the coatings including discoloration, chalking, etc. was observed (Figure S3).

3. Results and Discussion

3.1. The Structural Characterization of SiO$_2$ and KH560/SiO$_2$

The FT-IR spectra of SiO$_2$ and KH560/SiO$_2$ can offer structural information, as shown in Figure 2. The FT-IR spectra of SiO$_2$ shows typical peaks at 3433, 1638, and 1095 cm^{-1}, which are attributed to O-H anti-symmetric stretching, H-O-H bending vibration, and Si-O-Si anti-symmetric stretching, respectively. The strong and sharp peaks at 798 and 466 cm^{-1} belong to the Si-O bending vibration. KH560/SiO$_2$ shows some special peaks in contrast with the FT-IR spectra of SiO$_2$. Characteristic peaks at 2925 and 2852 cm^{-1} can be observed [24], which belong to the stretching vibration peaks of -CH$_3$ and -CH$_2$- from the organic silane coupling agent (KH560). The results show that the introduction of KH560 to the surface of the SiO$_2$ was successful.

The thermal properties of SiO$_2$ and KH560/SiO$_2$ were measured by TGA under an N$_2$ atmosphere and are shown in Figure 3. The results of all samples displayed a significant weight loss of about 5% from 150 °C, which can be ascribed to the decomposition of the free adsorption of water and the unstable oxygen functional groups of carbonyl and carboxyl. As the temperature increased, the decomposition of SiO$_2$ decreased slowly and the corresponding residual rate was 96.9% at 800 °C. Moreover, the KH560/SiO$_2$ began to show significant decomposition during the heating process. The initial thermal decomposition temperature of KH560/SiO$_2$ was 200 °C. The silane coupling agents (KH560) contained lower heat resistance bonds of the methylene group (-CH$_2$) and ether bond (-O-), which caused decomposition and exhibited a remarkable thermal weight loss after introduction on the surface of the SiO$_2$. The residual rate of KH560/SiO$_2$ was 88.5%. The introduction of KH560 bonds led to a sharp decomposition decline from the curves of KH560/SiO$_2$ and showed the successful preparation of KH560/SiO$_2$.

3.2. Effect of P:E and P:E:K Ratios on the Preparation and Properties of PEDOT:PSS/Epoxy and PEDOT:PSS/Epoxy/(KH560/SiO$_2$)

3.2.1. Preparation and Properties of PEDOT:PSS/Epoxy and PEDOT:PSS/Epoxy/(KH560/SiO$_2$) Composite Aqueous Dispersions

Strong hygroscopicity, subpar mechanical properties, and other drawbacks could inhibit the electronic applications of PEDOT:PSS coatings [26]. On the other hand, epoxy resins have been widely employed with other conductive fillers to provide excellent and long-lasting antistatic effects due to their highly cross-linked network structures, with the aid of curing reagents [27], as well as benefits such as moisture-proofing, wear-resistance, dust-proofing, surface smoothing, and good surface adhesion to various substrates. In this study, to achieve uniform mixing with PEDOT:PSS aqueous dispersion, the addition of a biobased waterborne curing agent into the waterborne epoxy emulsion (Table S1) is necessary for a strengthened emulsification. It is also worth noticing that the pre-mixing process of the waterborne epoxy emulsion and biobased curing agent should be completed as soon as possible to avoid a fast cross-linking curing reaction. According to Figure 1 (route 1), besides pristine PEDOT:PSS (P:E ratio = 1:0), there are ten dark-blue to gray-blue aqueous dispersions of PEDOT:PSS/epoxy prepared with P:E ratios ranging from 1:1 to 1:10, as shown in Figure S1.

Epoxy resins are kinds of synthetic resin with good mechanical properties, and the presence of an aromatic skeleton reduces its UV stability. After a long exposure to outdoor sunlight, an epoxy resin coating will lose its luster, yellowing, and chalking and will experience other defects, thus losing its ability to protect the base material. Since nano-SiO$_2$ is at the ultra-fine nanoscale with a size range of 1~100 nm, it has many unique

properties, such as optical properties against ultraviolet rays, aging resistance, strength and chemical resistance to other materials, being non-toxic, and not being harmful to the environment. Numerous investigations have been conducted on the mechanical characteristics of polymers augmented by nanofillers [28]. The modification of nano-SiO_2 can improve the compatibility and dispersion in polymer resin substrates, as well as improve the hardness and weatherability of the substrates and reduce the amount of film-former used, thus reducing costs. In addition, PEDOT:PSS is already highly UV-resistant, and the addition of nano-SiO_2 will synergistically enhance the UV resistance of the composite coating.

In view of the consequences of P:E ratios on the properties of PEDOT:PSS/epoxy coatings mentioned in the following sections, PEDOT:PSS/epoxy (P:E ratio = 1:4) was selected as the polymeric system and combined with SCA-modified SiO_2 (KH560/SiO_2) to further improve their weather resistance and mechanical properties. As shown in Figure 1, under alkaline conditions in ammonia, the nano-SiO_2 underwent a grafting reaction with the silane coupling agent via the silicone hydroxyl group. Such active organic groups could help with mixing compatibility and grafting or polymerizing with some polymers, for example, the epoxy curing agent [29]. Thus, it has been used as an additive and/or cross-linking agent in diverse coatings to improve their chemical resistance and mechanical properties.

For the preparation (Figure 1, route 2), PEDOT:PSS aqueous dispersion was firstly mixed with KH560/SiO_2 under high-speed shear emulsification to obtain a homogenized PEDOT:PSS/(KH560/SiO_2) dispersion. Then, the pre-prepared waterborne epoxy emulsion was mixed with it to achieve a series of PEDOT:PSS/epoxy/(KH560/SiO_2) ternary systems, in which the amount of PEDOT:PSS (10.00 ± 0.02 g, liquid weight) and P:E ratios (P:E ratio = 1:4) were kept fixed, while the effect of different levels of KH560/SiO_2 on the composite coating was investigated by controlled univariate experiments and dispersions with P:E:K of 1:4:0.05, 1:4:0.10, 1:4:0.15, 1:4:0.20, 1:4:0.25, and 1:4:0.30 were prepared. These aqueous dispersions had nearly the same look as PEDOT:PSS/epoxy dispersions, as was to be predicted, and their various components demonstrated relatively high compatibility to suit the following sample processing need.

3.2.2. Preparation and Morphology Properties of PEDOT:PSS/Epoxy and KH560/SiO_2 Composite Coatings

As shown in Figure 4 (inset), all the PEDOT:PSS/epoxy coatings with different P:E ratios exhibited a dark blue color and uniform appearance just like that of pristine PEDOT:PSS coating (Figure 4 inset). As shown in the microscope photos (Figure 4), it can be observed that the surface morphology of the pristine PEDOT:PSS coating exhibited a discrete dendritic distribution. The coating under an optical microscope exhibited a significant shift in color as the epoxy concentration rose. Such phenomena may originate from the aggregation trend of PEDOT:PSS macromolecular chains into large spherical composite particles in a polymer composite or the self-aggregation trend during the drying process [30], resulting in a darkening of the color. With the continuous increase in the epoxy ratios, composite coatings (P:E ratio ranging from 1:4 to 1:10) showed much denser and rougher states but without phase separation, together with gradually decreased surface electrical conductivity, as discussed below. The cause for that was that the cross-linking degree of composite polymer systems increased rapidly depending on the reaction between the epoxy resins and the amine curing agent, and the excellent compatibility between cured epoxy resin and PEDOT:PSS, but the deeply entangled distribution and encapsulated state by nonconducting epoxy resin chains will obstruct the conductive channel of PEDOT:PSS chains. To observe these composite coatings more clearly, the metallographic microscope was switched to an upper light source, so the photomicrograph of the coatings appeared yellow (Figures 5 and 7).

The preparation method of PEDOT:PSS/epoxy/(KH560/SiO_2) coatings was the same as that of PEDOT:PSS/epoxy coatings. As shown in Figures 6 and 7, all the PEDOT:PSS/epoxy/(KH560/SiO_2) coatings exhibited similar, uniform, and compact morphologies, just

like that of PEDOT:PSS/epoxy (P:E ratio = 1:4) in Figures 4 and 5. Under a microscope, with the increase in KH560/SiO$_2$, the coating's color deepened in certain spots, but no sizable darkened regions were visible, demonstrating that a relatively homogeneous mixing of KH560/SiO$_2$ with PEDOT:PSS/epoxy was accomplished.

To further demonstrate that both composite systems achieve a more homogeneous mixing, the PEDOT:PSS/epoxy coating (P:E ratio = 1:4) and the PEDOT:PSS/epoxy/(KH560/SiO$_2$) coatings (P:E:K = 1:4:0.15) were chosen for SEM structural analysis (Figure 8a,c). EDS mapping (Figure 8b,d) was then used to show the homogeneous distribution of PEDOT:PSS in epoxy for S elements and for Si elements of KH560/SiO$_2$ in PEDOT:PSS/epoxy. The SEM picture reveals that the structural chains of the PEDOT:PSS molecules were in touch with one another in the epoxy substrate and eventually created a conductive channel, whereas KH560/SiO$_2$ was primarily contained in the PEDOT:PSS/epoxy substrate. With the aid of EDS mapping, the homogeneous distribution of S elements in PEDOT:PSS further demonstrated the homogeneous mixing of PEDOT:PSS/epoxy; The majority of the Si elements in KH560/SiO$_2$ were homogeneously dispersed in the PEDOT:PSS/epoxy substrate, with a small amount of Si aggregation, which confirms the relatively homogeneous mixing of the PEDOT:PSS/epoxy/(KH560/SiO$_2$).

To observe the molecular structure changes in the PEDOT:PSS/epoxy system, FT-IR was used to characterize it. The absorption peak at 916 cm^{-1} in Figure 9 was attributed to the stretching vibration of the epoxy ring of PEDOT:PSS/epoxy just like that in uncured epoxy resin; nothing but the peak strength was weakened owing to the ring-opening reaction of the epoxy group after the addition of the biobased amine curing agent [31]. The existences of PEDOT:PSS in the PEDOT:PSS/epoxy composite coating can also be indicated due to the presence of peaks at 1636 and 1401 cm^{-1}, which belong to the C-C and C=C stretching vibrations of the quinoidal structure of the thiophene ring. The bands that existed at 831 cm^{-1} were related to the C-S stretching of the thiophene ring. Moreover, the intense peak at 1035 cm^{-1} corresponded to the stretching vibrations of C-O-C in the ethylenedioxy group, while the peak located at 1185 cm^{-1} was associated with the asymmetric and symmetric vibrations of S-O in the sulfonate groups of the PSS chains [32]. As described above, the weakening of the absorption peak belonging to the epoxy ring in PEDOT:PSS/epoxy proved that the composite system has been successfully cross-linked.

3.2.3. Bulk Resistance Property of PEDOT:PSS/Epoxy and PEDOT:PSS/Epoxy (KH560/SiO$_2$) Coatings

As shown by the bulk resistance data listed in Figure 10, after combination with epoxy resin, the electrically conductive property of PEDOT:PSS/epoxy coatings showed a downward trend according to the decreased P:E ratios. In detail, the bulk resistance logarithmic curve for P:E from 1:1 to 1:3 exhibited a linear rise (the 10^3 to 10^6 Ω level). In contrast, for P:E from 1:4 to 1:7, the resistance increase slowed down (the 10^6 to 10^7 Ω level) until it ultimately surpassed the instrument's range under a P:E ratio of 1:8 (out of the instrument range). The primary causes for these results are the dispersion effect and obstruction interaction of the PEDOT:PSS-based conductive channels from cured epoxy resin chains and cross-linked network, as well as the potential impact of -NH$_2$ in epoxy curing agent structures on the anion doping level of PEDOT$^+$, which is its conductive base.

Although the establishment of conductive channels was somewhat inhibited as the KH560/SiO$_2$ percentage rose, within a specific range, the bulk resistance of the composite coating fluctuated a little within the antistatic level (the 10^6 to 10^7 Ω level) and only increased by one order of magnitude (P:E:K ratios ranging from 1:4:0.05 to 1:4:0.30), demonstrating that it may be applied in antistatic applications. This also proved the good combination and uniform distribution of three kinds of components in the coatings of PEDOT:PSS/epoxy/(KH560/SiO$_2$) from the side.

3.2.4. Surface Wettability and Water Resistance of PEDOT:PSS/Epoxy and PEDOT:PSS/Epoxy/(KH560/SiO$_2$) Coatings

Due to the existence of PSS chains, PEDOT:PSS can be dispersed in water, and despite its coating being difficult to be re-dispersed, it shows a considerable hygroscopic capability, which results in the swelling of molecular chains and thus dramatically interferes with its structural, mechanical, electrical, and other properties [5]. Since the cross-linked dense structure of epoxy resins plays a role in resisting water absorption, here, the effects of P:E ratios on the change in WCAs of the PEDOT:PSS/epoxy coatings were investigated.

Theoretically, WCAs are controlled both by the surface energy and roughness of the coating [33]. A low surface energy (i.e., the presence of silicon- or fluorine-containing functional groups) or a rougher surface means a much more hydrophobic surface. As shown in Figure 11, there is generally one stage for the effect of P:E ratios on the WCAs. With the combination of epoxy resin and PEDOT:PSS, the hydrophilicity of the composite coating tended to be weakened in comparison with both the pristine PEDOT:PSS (P:E = 1:0) and pure epoxy (P:E = 0:1) coatings.

As shown in Figure 11a, the WCAs fluctuated between 79.6° and 83.8° when the P:E changed from 1:1 to 1:10, and the wetting capabilities of the composite system were somewhat diminished in comparison with the pure PEDOT:PSS and epoxy coatings. One reason is that, after the mechanical mixing and drying processes, the PEDOT:PSS/epoxy coatings showed a slightly frosted surface, resulting in improved roughness in contrast to the pure coatings of both. On the other hand, PEDOT:PSS undergoes significant aggregation with increasing epoxy, which may result in a P:E ratio with a rougher surface. This is consistent with the abovementioned morphology results shown in Figures 4 and 5.

As shown in Figure 11b, the WCAs of the coating with a P:E:K of 1:4:0.05 initially exhibited a minor reduction compared to that of the coating with a P:E of 1:4, which is due to the high hydrophilicity of nano-SiO$_2$. After that, it could be because nano-SiO$_2$ particles, which have a diameter of around 30 nm, kept being added, increasing the coating's surface roughness. As a result, the coating's wettability decreased at a P:E:K ratio of 1:4:0.15. After that, the hydrophilicity of the nano-SiO$_2$ took dominance, and the coating's WCAs dropped from 83.5° to 74.9°, causing the composite coating to have a consistent WCA reduction with P:E:K ratios ranging from 1:4:0.15 to 1:4:0.30.

Even though all the composite coatings still exhibited hydrophilicity, as the water immersion experiment results show in Figure S2, relying on the robust cross-linking structure, the PEDOT:PSS/epoxy (P:E = 1:4) coating (as a representative) could maintain its structural stability and substrate adhesion even after 10 days. In comparison, the pristine PEDOT:PSS coating quickly swelled within 40 min and totally disintegrated and fragmented within 1 day. Such good "water rejection" at the bulk phase can partially make up for the drawback of surface hydrophilicity in practical use.

Meanwhile, by connecting organic functional groups to the surface of SiO$_2$, silane coupling agents improved the dispersion of SiO$_2$ in the polymer substrate coating while reducing its own tendency to aggregate [21,22]. Additionally, KH560/SiO$_2$ as a filler lengthens the distance at which water may penetrate where the coating and substrate contact. KH560/SiO$_2$ is intrinsically hydrophilic. Although it can increase the water resistance of the coating to a certain extent. It is, thus, necessary to conduct more research into how KH560/SiO$_2$ affects the coating's water resistance. However, over the 10-day immersion period, the composite coatings with P:E:K ratios ranging from 1:4:0.05 to 1:4:0.30 showed good integrity and adherence to the substrate. These properties were highly dependent on the strengthened cross-linking structure and entanglement of KH560/SiO$_2$ with PEDOT:PSS/epoxy components.

3.2.5. Pencil Hardness Property of PEDOT:PSS/Epoxy and KH560/SiO$_2$ Composite Coatings

Due to the soft and organic nature of PEDOT:PSS, its coating has poor mechanical properties such as adhesion and hardness, which easily causes substrate detachment or

surface damage during its application lifetime. In this study, it was shown that composite coatings of PEDOT:PSS/epoxy could achieve higher mechanical characteristics than a pristine PEDOT:PSS coating through the cross-linking and curing reactions of the epoxy resin. It can be observed from Table 1 that, with the decrease in P:E ratios, the pencil hardness generally showed a significantly upward trend from the 3B to H levels, and the hardness of the composite coating fluctuated from HB to H, with P:E from 1:1 to 1:10. When further increasing the epoxy proportion, a much strong crosslinking system will be formed, as indicated in Figure 4, but the conductive paths will become discrete.

Table 1. The pencil hardness properties of PEDOT:PSS/epoxy coatings under different P:E ratios.

PEDOT:PSS/Epoxy	1:0	1:1	1:2	1:3	1:4	1:5	1:6	1:7	1:8	1:9	1:10	0:1
Hardness level	3B	H	HB	H	F	F	F	F	H	H	H	F

The data listed in Table 2 represent the effect of $KH560/SiO_2$ on the hardness properties of PEDOT:PSS/epoxy/($KH560/SiO_2$) coatings. It can be seen that the addition of $KH560/SiO_2$ brings certain benefits that improve the mechanical properties of PEDOT:PSS/epoxy coatings. Within a certain range, a high $KH560/SiO_2$ content means higher hardness. As can be seen from the data in Table 2, it was found that coatings with P:E:K ratios ranging from 1:4:0.05 to 1:4:0.30 all have a hardness level of H, demonstrating the hardness enhancing effect of SiO_2 on the composite coatings.

Table 2. The pencil hardness properties of PEDOT:PSS/epoxy/($KH560/SiO_2$) coatings under different P:E:K ratios.

PEDOT:PSS/Epoxy/($KH560/SiO_2$)	1:4:0.05	1:4:0.10	1:4:0.15	1:4:0.20	1:4:0.25	1:4:0.30
Hardness level	H	H	H	H	H	H

3.2.6. UV Resistance Properties of PEDOT:PSS/Epoxy and $KH560/SiO_2$ Composite Coatings

Epoxy resins are widely recognized for their vulnerability to UV deterioration in comparison with other materials such as polyurethanes, acrylics, polyesters, or alkyds. The breakdown of the polymeric structure as well as the staining and chalking of the coating layer can be caused by the aromatic moieties' absorption of UV light [17–19].

The 365.0 nm and 253.7 nm wavelengths of the triple-purpose UV analyzer were turned on simultaneously to speed up the aging experiment. A visual examination was used to assess the effectiveness of the PEDOT:PSS/epoxy and PEDOT:PSS/epoxy/($KH560/SiO_2$) composites for strong outdoor UV radiation. It was found that the pure epoxy coating sample experienced extreme oxidation under expedited circumstances. The samples' original hue turned to yellow as a result of oxidation.

As the aging experiment images show in Figure S3, comparatively speaking, neither the PEDOT:PSS/epoxy nor the PEDOT:PSS/epoxy/($KH560/SiO_2$) composite coatings had appreciable color changes. The color and shape of the composite coatings with a PEDOT:PSS/epoxy of 1:4 and a P:E:K from 1:4:0.05 to 1:4:0.30 were identical to those from 16 days prior, demonstrating the strong UV resilience of both the PEDOT:PSS and PEDOT:PSS/($KH560/SiO_2$) composites.

4. Conclusions

In this study, the aqueous dispersion of PEDOT:PSS was synthesized via a low-cost and facile technique and then combined with a waterborne epoxy emulsion together with a biobased curing reagent to form a homogeneous mixture using the simple mechanical blending method. The formed PEDOT:PSS/epoxy coatings with different P:E ratios meet excellent antistatic bulk resistance levels and have lower hydrophilicity. It was further

compounded with KH560/SiO$_2$, which not only helped to lower the cost by lowering the amount of film-forming material used but also contributed to improving the hardness of the composite coating (all PEDOT:PSS/epoxy/(KH560/SiO$_2$) samples had P:E:K ratios ranging from 1:4:0.50 to 1:4:0.30, bulk resistance levels between 10^6 and 10^7 Ω, a hardness level of H, the ability to withstand being submerged in water for 10 days without losing structural integrity, and good aging resistance under UV irradiation for 16 days). In conclusion, the essential mechanical qualities of the coating were provided by the epoxy resin as a film-former, while PEDOT:PSS and the modified SiO$_2$ collaborated to increase the epoxy coating's resistance to UV aging. The final high-hardness, UV-resistant aqueous conductive coating was created more affordably.

By improving self-made PEDOT:PSS aqueous dispersion (on solid content, particle size, etc.), using new composite components (such as bio-based epoxy resins, superhydrophobic macromolecules, etc.) and adjusting their composition ratios, or implementing new design methodologies (such as thermally reversible Diels-Alder groups, etc. to realize self-healing capability), many satisfied and thorough performances may be anticipated in the future. Additionally, display screens should take into account the thickness, color, and optical transparency of PEDOT-based conductive coatings to help develop new uses for PEDOTs:PSS and waterborne epoxy resin. The additional anti-corrosion effect of these conductive coatings can be anticipated if used on the metallic matrix, which will be quite promising in the shipping, automobile, electronic equipment, and aviation industries, among others, given the excellent electrochemical activity of PEDOT:PSS and the extensive benefits of epoxy resins.

Supplementary Materials: The following supporting information can be downloaded at: https://www.mdpi.com/article/10.3390/jcs7020051/s1, Figure S1: Photos of waterborne epoxy emulsion, biobased curing agent, and PEDOT:PSS/Epoxy aqueous dispersions with different P:E ratios; Figure S2: Water immersion experiment of PEDOT:PSS (0–1 day), PEDOT:PSS/Epoxy (P:E = 1:4) (0 day, 10 days), and PEDOT:PSS/Epoxy/(KH560/SiO$_2$) (0 days, 10 days) coatings; Figure S3: UV resistance experiment of Epoxy, PEDOT:PSS/Epoxy (P:E = 1:4), and PEDOT:PSS/Epoxy/(KH560/SiO$_2$) coatings with different P:E:K ratios; Table S1: Physical and chemical properties of the utilized materials.

Author Contributions: Z.L.: Conceptualization, Methodology, Software, Formal analysis, Investigation, and Writing—original draft; L.Z.: Revision and review; X.X.: Revision and review; M.Z.: Revision and review; C.F.: Resources and Supervision; S.C.: Conceptualization, Writing—review and revision, Supervision, and Project administration. All authors have read and agreed to the published version of the manuscript.

Institutional Review Board Statement: Not applicable.

Informed Consent Statement: Not applicable.

Data Availability Statement: The data presented in this study are available from the corresponding author upon request.

Conflicts of Interest: The authors declare no conflict of interest.

References

1. Fan, X.; Nie, W.Y.; Tsai, S.H.; Wang, N.X.; Huang, H.H.; Cheng, Y.J.; Wen, R.J.; Ma, L.J.; Yan, F.; Xia, Y.G. PEDOT:PSS for Flexible and Stretchable Electronics: Modifications, Strategies, and Applications. *Adv. Sci.* **2019**, *6*, 1900813. [CrossRef] [PubMed]
2. Liao, J.J.; Si, H.W.; Zhang, X.D.; Lin, S.W. Functional Sensing Interfaces of PEDOT:PSS Organic Electrochemical Transistors for Chemical and Biological Sensors: A Mini Review. *Sensors* **2019**, *19*, 218. [CrossRef] [PubMed]
3. Gao, N.; Yu, J.R.; Tian, Q.Y.; Shi, J.F.; Zhang, M.; Chen, S.; Zang, L. Application of PEDOT:PSS and Its Composites in Electrochemical and Electronic Chemosensors. *Chemosensors* **2021**, *9*, 79. [CrossRef]
4. Xia, Y.J.; Yan, G.W.; Lin, J. Review on Tailoring PEDOT:PSS Layer for Improved Device Stability of Perovskite Solar Cells. *Nanomaterials* **2021**, *11*, 3119. [CrossRef]
5. Zhu, D.L.; Miao, M.; Du, X.J.; Peng, Y.Y.; Wang, Z.; Liu, S.J.; Xing, J.F. Long/Short chain Crosslinkers-optimized and PEDOT:PSS-enhanced covalent double network hydrogels rapidly prepared under green LED irradiation as flexible strain sensor. *Eur. Polym. J.* **2022**, *174*, 111327. [CrossRef]
6. Yang, Y.; Zhao, G.J.; Cheng, X.; Deng, H.; Fu, Q. Stretchable and Healable Conductive Elastomer Based on PEDOT:PSS/Natural Rubber for Self-Powered Temperature and Strain Sensing. *ACS Appl. Mater. Inter.* **2021**, *13*, 14599–14611. [CrossRef]
7. Tan, Z.T.; Li, H.W.; Huang, Y.N.; Gong, X.; Qi, J.N.; Li, J.; Chen, X.S.; Ji, D.Y.; Lv, W.B.; Li, L.Q.; et al. Breathing-effect assisted transferring large-area PEDOT:PSS to PDMS substrate with robust adhesion for stable flexible pressure sensor. *Compos. Part. A Appl. Sci. Manuf.* **2021**, *143*, 106299. [CrossRef]
8. Huang, J.M.; Ren, Z.W.; Zhang, Y.K.; Liu, K.; Zhang, H.K.; Tang, H.; Yan, C.Q.; Zheng, Z.J.; Li, G. Stretchable ITO-Free Organic Solar Cells with Intrinsic Anti-Reflection Substrate for High-Efficiency Outdoor and Indoor Energy Harvesting. *Adv. Funct. Mater.* **2021**, *31*, 2010172. [CrossRef]
9. Zhao, X.; Wang, W.L.; Wang, Z.; Wang, J.N.; Huang, T.; Dong, J.; Zhang, Q.H. Flexible PEDOT:PSS/polyimide aerogels with linearly responsive and stable properties for piezoresistive sensor applications. *Chem. Eng. J.* **2020**, *395*, 125115. [CrossRef]
10. Cho, H.S.; Jang, E.; Liu, H.; Cho, G. Applicability of poly(3,4-ethylenedioxythiophene): Poly(styrene sulfonate) impregnated polyurethane nanoweb as a transmission line for smart textiles. *Text. Res. J.* **2021**, *91*, 1253–1262. [CrossRef]
11. Zhang, R.; Wang, Y.; Li, J.; Zhao, H.; Wang, Y.; Zhou, Y. Mesoporous cellulose nanofibers-interlaced PEDOT:PSS hybrids for chemiresistive ammonia detection. *Microchim. Acta* **2022**, *189*, 308. [CrossRef]
12. Si, P.X.; Trinidad, J.; Chen, L.; Lee, B.; Chen, A.; Persic, J.; Lyn, R.; Leonenko, Z.; Zhao, B.X. PEDOT:PSS nano-gels for highly electrically conductive silver/epoxy composite adhesives. *J. Mater. Sci. Mater. Electron.* **2018**, *29*, 1837–1846. [CrossRef]
13. Zeng, F.J.; Zhao, X.; Luo, M.Y.; Wang, W.; Qing, X.; Lu, Y.; Zhong, W.B.; Liu, Q.Z.; Luo, J.; Li, M.F.; et al. A transparent PEDOT:PSS/PVA-co-PE/epoxy thermoelectric composite device with excellent flexibility and environmental stability. *Compos. Sci. Technol.* **2022**, *218*, 109153. [CrossRef]
14. Wu, Y.Q.; He, Y.; Zhou, T.G.; Chen, C.L.; Zhong, F.; Xia, Y.Q.; Xie, P.; Zhang, C. Synergistic functionalization of h-BN by mechanical exfoliation and PEI chemical modification for enhancing the corrosion resistance of waterborne epoxy coating. *Prog. Org. Coat.* **2020**, *142*, 105541. [CrossRef]
15. Li, W.; Xu, G.L.; Xu, B.Q.; Wang, Y.; Yang, J.; Hu, J. Preparation of waterborne P-N containing epoxy resin curing and its performances. *Pigm. Resin. Technol.* **2016**, *45*, 308–312. [CrossRef]
16. Sun, J.; Zhang, Z.P.; Wang, L.; Liu, H.; Ban, X.Y.; Ye, J.J. Investigation on the epoxy/polyurethane modified asphalt binder cured with bio-based curing agent: Properties and optimization. *Constr. Build. Mater.* **2022**, *320*, 12. [CrossRef]
17. Khotbehsara, M.M.; Manalo, A.; Aravinthan, T.; Turner, J.; Ferdous, W.; Hota, G. Effects of ultraviolet solar radiation on the properties of particulate-filled epoxy based polymer coating. *Polym. Degrad. Stabil.* **2020**, *181*, 109352. [CrossRef]
18. Noe, C.; Hakkarainen, M.; Sangermano, M. Cationic UV-Curing of Epoxidized Biobased Resins. *Polymers* **2021**, *13*, 89. [CrossRef]
19. Wang, X.Q.; Fan, H.N.; Li, W.R.; Zhang, Y.Y.; Shang, R.Q.; Yin, F.H.; Wang, L.M. Effect of Ultraviolet-A Radiation on Alicyclic Epoxy Resin and Silicone Rubber Used for Insulators. *Polymers* **2022**, *14*, 4889. [CrossRef]
20. Zaghloul, M.Y.; Zaghloul, M.M.Y.; Zaghloul, M.M.Y. Influence of stress level and fibre volume fraction on fatigue performance of glass fibre-reinforced polyester composites. *Polymers* **2022**, *14*, 2662. [CrossRef]
21. Vu, C.M.; Bach, Q.V.; Duong, L.X.; Thai, N.V.; Thao, V.D.; Duc, P.T.; Nguyen, D.D.; Hoang, T.; Van, T.N. Silane coupling agent with amine group grafted nano/micro-glass fiber as novel toughener for epoxy resin: Fabrication and mechanical properties. *Compos. Interfaces* **2020**, *27*, 1085–1100.
22. Wahyuningsih, K.; Yuliani, S.; Hoerudin. Characteristics of Silica Nanoparticles from Rice Husk as Influenced by Surface Modification with Used Solvent Containing Silane. *J. Eng. Technol. Sci.* **2021**, *53*, 11. [CrossRef]
23. Gao, Z.L.; Gao, T.; Geng, Q.; Lin, G.L.; Li, Y.F.; Chen, L.; Li, M.C. Improving light absorption of active layer by adjusting PEDOT:PSS film for high efficiency Si-based hybrid solar cells. *Sol. Energy* **2021**, *228*, 299–307. [CrossRef]
24. Hu, L.Q.; Pu, Z.J.; Tian, Y.H.; Zheng, X.Y.; Cheng, J.; Zhong, J.C. Preparation and properties of fluorinated silicon two-component polyurethane hydrophobic coatings. *Polym. Int.* **2020**, *69*, 448–456. [CrossRef]
25. Chen, S.; Lu, B.Y.; Xu, J.K.; Qin, L.Q.; Wang, Z.P.; Duan, X.M. Preparation and characterization of aqueous dispersions of poly(3,4-ethylenedithiathiophene-co-3,4-ethylenedioxythiophene)/ poly(styrene sulfonate) and their conducting films. *J. Appl. Polym. Sci.* **2013**, *129*, 1717–1725. [CrossRef]
26. Xin, X.; Yu, J.R.; Gao, N.; Xie, X.W.; Chen, S.; Zhong, J.; Xu, J.K. Effects of POSS composition on PEDOT:PSS conductive film. *Synth. Met.* **2021**, *282*, 116947. [CrossRef]

27. Gao, W.; Dang, Z.C.; Liu, F.S.; Wang, S.; Zhang, D.W.; Yan, M.X. Preparation of antistatic epoxy resin coatings based on double comb-like quaternary ammonium salt polymers. *RSC Adv.* **2020**, *10*, 43523–43532. [CrossRef] [PubMed]

28. Zaghloul MY, M.; Zaghloul MM, Y.; Zaghloul MM, Y. Developments in polyester composite materials–An in-depth review on natural fibres and nano fillers. *Compo. Struct.* **2021**, *278*, 114698. [CrossRef]

29. Chi, H.; Zhang, G.C.; Wang, N.; Wang, Y.G.; Li, T.D.; Wang, F.K.; Ye, C. Enhancing the mechanical strength and toughness of epoxy resins with linear POSS nano-modifiers. *Nanoscale Adv.* **2022**, *4*, 1151–1157. [CrossRef]

30. Matsubayashi, T.; Tenjimbayashi, M.; Manabe, K.; Komine, M.; Navarrini, W.; Shiratori, S. Integrated Anti-Icing Property of Super-Repellency and Electrothermogenesis Exhibited by PEDOT:PSS/Cyanoacrylate Composite Nanoparticles. *ACS Appl. Mater. Inter.* **2016**, *8*, 24212–24220. [CrossRef]

31. Parshina, M.S.; Tarasenkov, A.N.; Aysin, R.R.; Tebeneva, N.A.; Buzin, M.I.; Afanasyev, E.S.; Serenko, O.A.; Muzafarov, A.M. Monitoring the curing processes of epoxy oligomers with partially substituted polyethoxymetallosiloxanes by IR spectroscopy and thermomechanical analysis. *J. Appl. Polym. Sci.* **2021**, *138*, 50918. [CrossRef]

32. Aycan, D.; Dolapci, N.; Karaca, O.G.; Alemdar, N. Polysaccharide-based electroconductive films for controlled release of ciprofloxacin. *J. Appl. Polym. Sci.* **2022**, *139*, e52761. [CrossRef]

33. Zhang, L.S.; Zhou, A.G.; Sun, B.R.; Chen, K.S.; Yu, H.Z. Functional and versatile superhydrophobic coatings via stoichiometric silanization. *Nat. Commun.* **2021**, *12*, 7. [CrossRef] [PubMed]